MOLECULAR AND CELLULAR BIOLOGY, Dec. 2005, p. 10604–10610 Vol. 25, No. 23
0270-7306/05/$08.00+0 doi:10.1128/MCB.25.23.10604–10610.2005


# The Murine Stanniocalcin 1 Gene Is Not Essential for Growth and Development

Andy C.-M. Chang,[1] Jeon Cha,[1] Frank Koentgen,[2]† and Roger R. Reddel[1]*

*Children's Medical Research Institute, 214 Hawkesbury Road, Westmead, NSW 2145, Australia,*[1] *and Walter and Eliza Hall Institute of Medical Research, Parkville, VIC 3050, Australia*[2]

Received 17 June 2005/Returned for modification 11 July 2005/Accepted 10 September 2005

**The stanniocalcin 1 (STC1) gene is expressed in a wide variety of tissues, including the kidney, prostate, thyroid, bone, and ovary. STC1 protein is considered to have roles in many physiological processes, including bone development, reproduction, wound healing, angiogenesis, and modulation of inflammatory response. In fish, STC1 is a hormone that is secreted by the corpuscles of Stannius and is involved in calcium and phosphate homeostasis. To determine the role of STC1 in mammals, we generated *Stc1*-null mice by gene targeting. The number of *Stc1*$^{-/-}$ mice obtained was in accordance with Mendelian ratios, and both males and females produced offspring normally. No anatomical or histological abnormalities were detected in any tissues. Our results demonstrated that *Stc1* function is not essential for growth or reproduction in the mouse.**

Stanniocalcin 1 (STC1) is a glycoprotein that was first identified in fish as a hormone secreted by the corpuscles of Stannius, an organ unique to bony fish. It is secreted into the blood in response to elevated calcium and has potent activity on the gills, kidneys, and gut to regulate calcium absorption and phosphate excretion (8, 16, 17). We and others have identified two related mammalian genes encoding STC1 and STC2 that are paralogs of the fish gene (2, 4, 6, 11, 20, 21). Mammalian STCs are expressed in a wide variety of tissues, including the kidney, ovary, prostate, thyroid, and spleen.

Given its role in fish, initial functional analyses of mammalian STC1 focused on determining whether its role in regulating blood calcium has been conserved. In vivo studies in which recombinant STC1 protein was injected into rats indicated that STC1 may regulate blood calcium by increasing renal reabsorption of phosphate, and in vitro experiments showed that STC1 could reduce the flux of calcium across the intestines of rats and swine while increasing absorption of phosphate (19, 21, 27). Interestingly, expression studies showed strong STC1 production in a variety of tissues during murine development and a general down-regulation of expression during postnatal development in all tissues except the ovary, where expression increased. On the basis of these and a variety of other functional and expression studies, it has been proposed that the physiologic roles of STC1 are pleiotropic and include early musculoskeletal development, female reproduction, cell motility, and a cytoprotective role in response to different stressors (13–15, 22, 24, 31–34). Moreover, evidence is also accumulating for a role of STC1 in cancer (reviewed in reference 3).

To determine whether STC1 plays a crucial role during normal development and provide a model for examining the function of STC1 in vivo, we generated mice that are null for STC1. We generated two independent lines (L278 and L282) by homologous recombination and examined them for overt abnormalities.

## MATERIALS AND METHODS

**Targeting vector construction and generation of *Stc1*-deficient mice.** Genomic DNA encoding STC1 was isolated from a mouse 129 SVJ Lambda FIXII library (Stratagene). Various inserts from positive lambda isolates were then subcloned into vector pGEM5Zf+ (Promega) for DNA sequencing. A 2.9-kb right targeting arm was obtained by PCR of lambda clones with two primers, A630 (5′-CCG CTCGAGCCTCTTCTTCACAGCATGGGG) and A631 (5′-CGGGGTACC TAGCCATTGCCATATATTTACTGAGCACCC) containing a XhoI and KpnI restriction site, respectively, and inserted into the KpnI-XhoI site of ploxPneo-1 (23) to generate plasmid pAC242. A 2.5-kb left arm was obtained by PCR of lambda clones with two primers, A749 (5′-GCGCGGATCCGCTCTATTCCT GCATAAAACC) and A629 (5′-TCCCCCGGGTCTCTGAGAAGTTTCCGC TAAGTTG) containing BamHI and SmaI restriction site, respectively, and then inserted into the BamHI-SmaI site of pAC242 to generate pAC248. The left targeting arm contained 5′ sequences plus the 5′ untranslated region of exon 1, including nucleotide −2 upstream of the ATG start codon of exon 1. The targeting construct, pAC248, was linearized with BamHI and electroporated into embryonic stem (ES) cells. Genomic DNA isolated from about 400 G418-resistant ES cell colonies was analyzed by Southern blotting. Two correctly targeted ES cell clones were identified and injected into blastocysts to generate chimeras and gave rise to two independent lines, L278 and L282. Chimeras were subsequently mated to C57BL/6 females, and the resulting heterozygous animals were bred to generate wild-type, *Stc1*$^{+/-}$, and *Stc1*$^{-/-}$ animals for subsequent analyses. All animal work was performed in accordance with guidelines established by the Australian Code of Practice for the Care and Use of Animals for Scientific Purposes.

**PCR and Southern and Northern blot analyses.** Genomic DNA isolated from ES cells or mouse tails was digested with XbaI or NheI, separated through a 0.8% agarose gel (Roche) with Tris-borate-EDTA buffer at pH 7.5, and transferred onto BiodyneB membrane (Pall) by capillary action in 0.4 M NaOH for 3 to 4 h. Two flanking DNA fragments P1 and P3, outside the targeting region, were used as hybridizing probes for genotyping. Hybridization of XbaI-cut DNA with the 0.6-kb P1 probe gave a band of 5.1 kb with the wild-type allele, whereas correctly targeted mutant allele gave a band of 3.7 kb (see Fig. 1). Hybridization with the 0.5-kb P3 probe gave a 7-kb wild-type band and a 4-kb mutant band on DNA digested with NheI. The P1 fragment was obtained by PCR within *Stc1* intron 3 using primers A653 (5′-TTTTGCTGAAAGCACAAGCCTC) and A654 (5′-TAATGCTGCCTGACTCTGAGGG). The P3 fragment was generated by PCR from a region upstream of the *Stc1* gene using primers A1507 (5′-TAG CCGAATGCCAGAAAACGCC) and A1508 (5′-TCAAAGCCAAGTTCCTTC CCAGAAG). PCR was carried out using the Expand High Fidelity system (Roche). Following an initial denaturation step (94°C for 10 min), *Taq* polymer-

* Corresponding author. Mailing address: Children's Medical Research Institute, 214 Hawkesbury Road, Westmead, Sydney, NSW 2145, Australia. Phone: 61296872800. Fax: 61296872120. E-mail: rreddel@cmri.usyd.edu.au.

† Present address: Ozgene Pty Ltd., P.O. Box 1368, Canning Vale, WA 6970, Australia.

ase was added and 35 cycles of PCR were then performed (94°C for 1 min, 63°C for 1 min, and 72°C for 3 min) and ended with a cycle of 72°C for 15 min.

For reverse transcription-PCR (RT-PCR) of the transcript from the targeted locus, total RNA was first transcribed with RNase H-minus Moloney murine leukemia virus reverse transcriptase (Promega), and then PCR was performed with primer A1216 (5′-CGACCACCAAGCGAAACATC) derived from the neomycin resistance gene (*Neo*) and primer A1252 (5′-CAGGAGAGGCAG AATGACCACA) from *Stc1* exon 4. The amplified 0.8-kb product was gel purified and subjected to DNA sequencing with an internal primer, primer A1218 (5′-CCGAATATCATGGTGGAAAAT).

For RT-PCR of *Stc2* and glyceraldehyde phosphodehydrogenase (GAPDH), primer pair A1549 (5′-TGTGACCCTGGCTTTGGTGTTTG) and A1550 (5′-CGTGGGAGGTCTCTGTATGTTGG) and primer pair A1505 (5′-ACC ACAGTCCATGCCATCAC) and A1506 (5′-TCCACCACCCTGTTGCTGTA) were used, respectively. One microgram of total RNA isolated from various mouse organs was reverse transcribed with RNase H-minus Moloney murine leukemia virus reverse transcriptase in a total volume of 50 μl. After synthesis, 5 μl and 2 μl of cDNA were used for PCR of *Stc2* and GAPDH sequences, respectively. For *Stc2* PCR, following an initial denaturation step (95°C for 10 min), *Taq* polymerase (Roche) was added, and the cDNA was amplified for 30 cycles (95°C for 50 s, 60°C for 30 s, and 72°C for 1 min). GAPDH cDNA was amplified for 20 cycles.

For Northern blotting, 10 μg of total RNA from mouse tissues was subjected to electrophoresis on a 1% formaldehyde gel, transferred to a Magna nylon membrane (Osmonics) by capillary action, and cross-linked by UV irradiation. Hybridization and washing conditions were as recommended by the manufacturer.

All probes for hybridization were labeled with [α-$^{32}$P]dCTP using the Gigaprime DNA labeling kit (Bresatec). A 3.2-kb exon 4-containing fragment was obtained by HindIII digestion of plasmid pAC224 that contained a 6.5-kb *Stc1* genomic DNA in pGEM5Zf+. The 3.2-kb fragment consisted of 360-bp intron 3 and 2.8-kb exon 4 sequences. A 2-kb *Neo*-specific fragment was obtained by digesting plasmid ploxPneo-1 with SalI and XbaI. A 300-bp cDNA that was specific for *Stc1* exon 2 and exon 3 was purified from plasmid pAC347 (that contained 0.9-kb *Stc1* cDNA) after digestion with NotI and HindIII.

**SDS-PAGE and Western blotting.** Mouse tissue samples (~4 mm$^3$) were processed with OMNI5000 homogenizer (Omni) in 1.5 ml lysis buffer (50 mM Tris-HCl [pH 8], 150 mM NaCl, 1% NP-40, 0.5% sodium deoxycholate, and 0.1% sodium dodecyl sulfate [SDS] and supplemented with Roche complete protease inhibitor and leupeptin). Particulate matter was pelleted by centrifugation, and the supernatant protein concentrations were determined with the bicinchoninic acid protein assay kit (Pierce). Proteins were resolved by SDS-polyacrylamide gel electrophoresis (PAGE) on 12% polyacrylamide gels and electrotransferred onto Immobilon P membranes (Millipore) for Western blotting. Membranes were probed with a goat STC1 antiserum raised against a peptide within an internal region of human STC1 (Santa Cruz Biotechnology) at a 1:500 dilution. Horseradish peroxidase-conjugated donkey anti-goat antibody was used as secondary antibody at a 1:4,000 dilution. Protein bands were visualized by using Supersignal West Pico chemiluminescence kit (Pierce) on SuperRX Fuji film.

**Histology, radiography, and body composition analyses.** Mice were euthanized by $CO_2$ inhalation, and necropsies were performed. Organs were fixed in 10% formalin and sent to a veterinary pathologist for sectioning and examination. Skeletal radiography of whole animals was performed on the B7070 Mammoview mammographic system (General Electric) after the animals were anesthetized with intraperitoneal injections of ketamine/xylazine. Total body fat and bone mineral density were determined using dual-energy X-ray absorptiometry (Lunar PIXImus2; General Electric Medical Systems) as described by the manufacturer.

**Treadmill performance.** Skeletal muscle function was evaluated from treadmill performance following a published protocol (30). Measurements were done on a mouse exercise treadmill equipped with a shock plate (Columbus Exer-4/8) at a linear velocity of 29 m/min and a 13° incline (aerobic exercise). Seven-week-old wild-type and *Stc1*$^{-/-}$ littermates were first trained for two 10-min intervals. Performance time was defined as the time the mice ran continuously without repeatedly falling back to the plate.

**Vitamin 1,25(OH)$_2$D$_3$ treatment and calcium and phosphate measurements.** Wild-type and *Stc1*$^{-/-}$ adult female mice were given intraperitoneal injections of vitamin 1,25(OH)$_2$D$_3$ (Calbiochem) at a dose rate of 2 μg/kg of body weight daily for 4 days. The mice were injected about an hour before the dark cycle. Animals were maintained on standard laboratory chow (Glen Forrest Stockfeeders) containing 0.77% calcium, 0.57% phosphorus, and 2,000 IU vitamin D/kg. On the morning after the last injection, the animals were anesthetized with halothane, and blood was collected from the heart. For baseline, a small amount of blood was collected from the tail a day before the start of injections. Measurements of calcium and inorganic phosphorus were made from clotted blood using Sigma diagnostic kits.

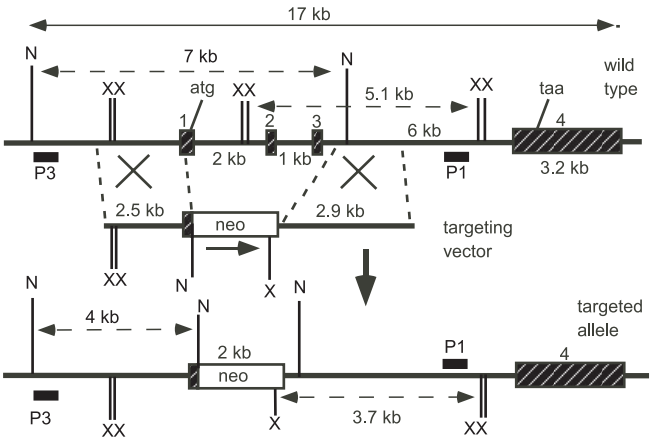


FIG. 1. Mouse *Stc1* locus, targeting vector, and targeted allele. The upper line shows a map of the *Stc1* locus with the four exons defined by the black hatched boxes. The XbaI (X) and NheI (N) restriction sites, protein initiation (atg) and termination (taa) codons are also indicated. The 3′ (P1) and 5′ (P3) external probes used for Southern blot analyses are shown. The diagnostic XbaI restriction fragments (5.1 kb and 3.7 kb) and NheI restriction fragments (7 kb and 4 kb) are shown with broken arrows.

## RESULTS

**Generation and confirmation of *Stc1*-deleted mice.** As a prelude to disrupting the *Stc1* gene, we isolated a 16-kb mouse genomic clone from a 129 SVJ lambda library. The gene was completely sequenced, and it has four exons (GenBank accession number AF512563). Exon 1 encodes the 5′ untranslated region and the first 39 amino acid residues of *Stc1* exon 2 encodes 48 residues, exon 3 encodes 71 residues, and exon 4 encodes the last 89 residues plus the 3′ untranslated region. The targeting vector was designed to delete the part of exon 1 that contains the first 39 residues of the N-terminal coding region and also exons 2 and 3 (Fig. 1). Correct deletion was first identified by Southern blot analysis with probe P1 that in wild-type animals showed a band of 5.1 kb, a band of 3.7 kb in *Stc1*$^{-/-}$ animals, and both bands in *Stc1*$^{+/-}$ animals (Fig. 2A). When the same Southern blot was stripped and reprobed with a 0.3-kb *Stc1* cDNA specific for exon 2 and exon 3, a band was seen in wild-type and *Stc1*$^{+/-}$ animals, and no band was seen in the *Stc1*$^{-/-}$ animals (Fig. 2B). This indicated that correct homologous recombination had occurred as planned in the *Stc1*$^{-/-}$ mice. This was further confirmed by Southern analysis of genomic DNA digested with NheI and probed with P3, a DNA fragment upstream of the left targeting arm. Wild-type DNA gave a 7-kb band, whereas *Stc1*$^{-/-}$ DNA gave a 4-kb band (Fig. 2C).

To confirm genomic deletion, Northern blot analysis was performed on RNA isolated from ovaries that are known to produce a high level of *Stc1* transcripts (26). The blot was probed with the 0.3-kb *Stc1* cDNA specific for exon 2 and exon 3. A 4-kb band was seen in wild-type animals as expected but

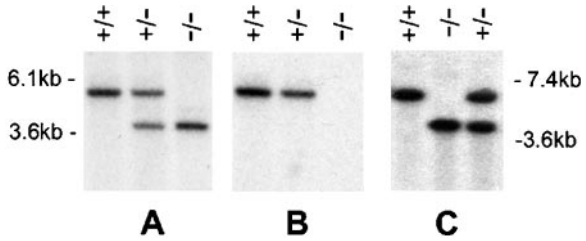


FIG. 2. Southern blot analysis of wild-type (+/+), heterozygous (+/−), and homozygous mutant (−/−) mice. (A) Tail DNA was digested with XbaI, transferred onto a BiodyneB membrane, and hybridized with radioactive probe P1. The predicted bands are seen for each genotype. (B) The membrane was stripped and rehybridized with a 0.3-kb cDNA probe specific for *Stc1* exons 2 and 3. No band is seen in the −/− lane, indicating targeting of the *Stc1* allele. (C) DNA was digested with NheI and hybridized with probe P3. The positions of DNA molecular size markers are indicated at the sides of the blots.

not in $Stc1^{-/-}$ animals, indicating that deletion had occurred (Fig. 3A).

When we hybridized a similar Northern blot with a 3-kb exon 4-specific probe, a 4-kb band was seen in wild-type samples as expected (Fig. 3B). However, an equally strong but slightly larger band was also seen in the $Stc1^{-/-}$ sample. We postulated that this band results from splicing of the neomycin resistance (*Neo*) transcript to the remaining exon 4 of *Stc1*. This conclusion was supported by hybridizing a duplicate Northern blot with a 2-kb probe generated from the *Neo* cassette. The probe hybridized only to the larger 4-kb band in the $Stc1^{-/-}$ sample and not to the wild-type sample (Fig. 3C). The smaller 1.4-kb band corresponds to the usual *Neo* transcript.

To further investigate the nature of the spliced product, total

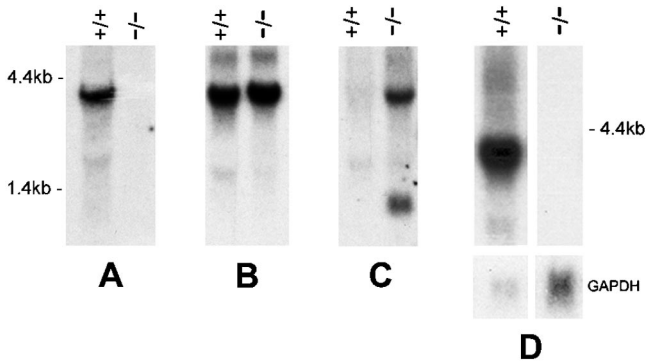


FIG. 3. Northern blot analysis of wild-type (+/+) and homozygous mutant (−/−) mice. (A) Ten micrograms of total RNA from ovaries was subjected to electrophoresis in a 1% formaldehyde gel, transferred to a Pall BiodyneB membrane, and hybridized with a 0.3-kb cDNA probe that was specific for exon 2 and exon 3. The *Stc1* transcript is seen only in the wild-type mice. (B) The blot was hybridized with a 3.2-kb exon 4-specific probe. While the correct transcript is seen in wild-type mice, an extraneous 4-kb band is seen in $Stc1^{-/-}$ mice. (C) The blot is a duplicate of that in panel B, but it was hybridized instead with a 2-kb *Neo*-specific probe. This probe hybridized to the novel 4-kb band, suggesting an aberrant splice *Neo-Stc1* exon 4 product. The lower 1.4-kb band is the usual *Neo* transcript. (D) RNA from ovaries isolated from wild-type and $Stc1^{-/-}$ L278nd mice (that had the *Neo* cassette deleted) were hybridized with *Stc1* cDNA. The novel 4-kb band is no longer present in the L278nd $Stc1^{-/-}$ mice. The lower panel shows hybridization to GAPDH as a loading control.

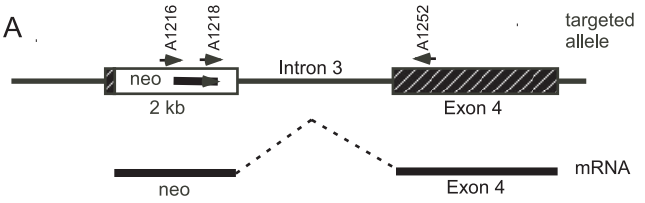


B

*CTCGTGCTTTACGGTATCGCCGCTCCCGATTCGCAGCGCA T*
*CGCCTTCTATCGCCTTCTTGACGAGTTCTTC **TGA**GGGGATC*
*GATCCGCT*ATACTACAACAGACTTGTCCGAAGCCTTCTGGA
ATG**TGATGA**AGACACGGTCAGTACAATCAGAGACAGC C**TGA**
TGGAGAAGATCGGGCC

FIG. 4. Sequence analysis of the novel transcript from the targeted allele. (A) The positions of the two RT-PCR primers A1216 and A1252 and the sequencing primer A1218 are indicated. The thicker line below represents the spliced product of the *Neo* transcript and exon 4, with the intervening intron 3 region deleted. (B) DNA sequence of the Neo-exon 4 spliced product obtained with primer A1218. The italicized letters show sequence derived from the neomycin cassette, and the protein-coding sequence for the neomycin resistance gene is underlined with the termination codon in bold type. The nonitalicized letters are sequence derived from exon 4 of *Stc1*; the exon 4 sequence is out of frame in the transcript, and there are three additional stop codons (bold type).

RNA from an $Stc1^{-/-}$ animal was subjected to RT-PCR using a sense primer from the *Neo* gene and an antisense primer from exon 4 (Fig. 4A). A 0.8-kb product was obtained and sequenced. The DNA sequence (Fig. 4B) revealed that the larger 4-kb transcript seen in $Stc1^{-/-}$ animals consisted of intact *Neo* sequence joined to exon 4. The termination codon (TGA) of the *Neo* gene is still intact, and the *Stc1* sequence which follows is out of frame and contains two consecutive stop codons (TGA). It is therefore highly likely that only the neomycin resistance protein would be translated from this 4-kb transcript and that no *Neo-Stc1* exon 4 fusion protein would be produced. This supported the conclusion that no truncated STC1 protein is produced from the $Stc1^{-/-}$ allele.

Two independent mouse lines, L278 and L282, were generated with the *Stc1* allele deleted as described above. As the targeting vector used for homologous recombination contained a pair of loxP sites flanking the *Neo* cassette (23), we crossed L278 mice with *CMV-CRE* deleter mice (Jackson Laboratory). Progeny were screened for deletion of the *Neo* cassette, and subsequently, *CMV-CRE* mice were bred out to generate mice with only the *Stc1* deletion (data not shown). This line is designated L278nd (for *Neo* deleted). Northern blot analysis of RNA isolated from wild-type and $Stc1^{-/-}$ ovaries revealed the absence of any *Stc1* transcripts in the latter (Fig. 3D). This result confirmed our conclusion that the 4-kb RNA transcript seen in L278 and L282 lines is derived from a spliced *Neo-Stc1* product driven by the promoter in the *Neo* cassette.

**Western blot analysis.** Immunoblot analysis against STC1 protein was performed with a commercially available polyclonal antibody. A single protein band of about 32 kDa, which is the predicted size for STC1 protein, was seen in extract from $Stc1^{+/+}$ quadriceps muscle but not in $Stc1^{-/-}$ quadriceps (Fig. 5A). We had previously generated STC1 polyclonal antibodies but found them unsuitable for Western blot analysis due to high nonspecific cross-reactivity (unpublished results).

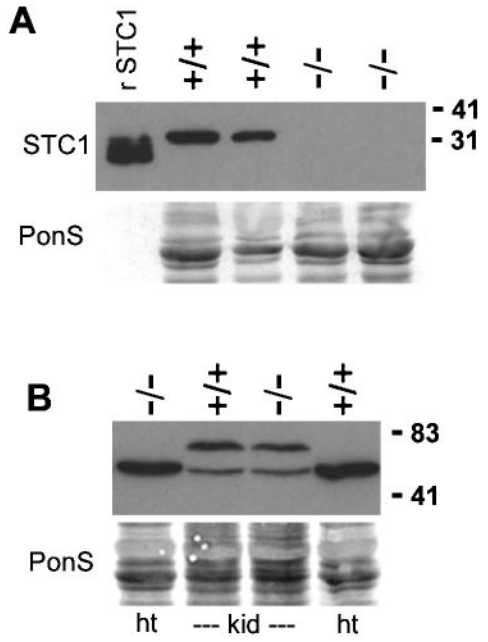


FIG. 5. Western blot analyses of STC1 protein from wild-type and $Stc1^{-/-}$ mice. (A) Total protein samples (30 μg) from quadriceps muscle of two wild-type (+/+) and two $Stc1^{-/-}$ (−/−) mice were resolved by SDS-PAGE and immunoblotted with STC1 polyclonal antibody. The leftmost lane contains 10 μg of purified human recombinant STC1 (rSTC1) protein produced by a baculoviral expression system (12). (B) Protein samples (30 μg) from heart (ht) and kidney (kid) were loaded. Cross-reactivities of this antibody are indicated by the presence of various bands that are larger than the STC1 bands in both wild-type and $Stc1^{-/-}$ tissues. Blots were stained for total proteins with Ponceau S (PonS) to indicate equal loads before immunoblotting was carried out. The positions of molecular mass markers (in kilodaltons) are indicated on the right.

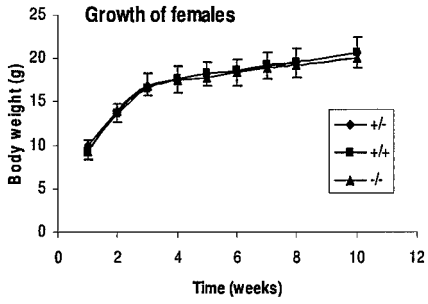


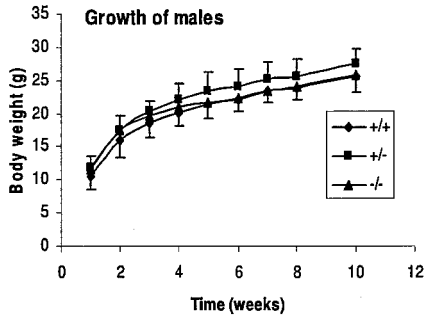


FIG. 6. Postnatal growth rate. The weights of female and male littermates were measured weekly after weaning (week 1). There were seven females of each genotype, seven $Stc1^{+/-}$ males, and six $Stc1^{+/+}$ and $Stc1^{-/-}$ males. Error bars indicate standard errors of the means.

When we further tested this polyclonal antibody on a variety of wild-type and $Stc1^{-/-}$ tissues, such as the heart and kidney, no 32-kDa band was seen (not shown), but there was some cross-reactivity with other larger proteins (Fig. 5B).

**Analysis of offspring from heterozygous breeding pairs.** Mice that carried one copy of the deleted gene were interbred to generate litters that were $Stc1^{+/+}$, $Stc1^{+/-}$, and $Stc1^{-/-}$ as determined by Southern blot analysis of DNA extracted from tail snips. Out of 226 pups born, 59 were $Stc1^{+/+}$, 99 were $Stc1^{+/-}$, and 68 were $Stc1^{-/-}$. This is close to the predicted Mendelian ratios of 1:2:1 expected for nondeleterious alleles. Thus, the *Stc1* knockout pups were no less viable than their wild-type littermates. The postnatal growth rates of wild-type, $Stc1^{+/-}$, and $Stc1^{-/-}$ male and female mice over a 10-week period were indistinguishable (Fig. 6). The $Stc1^{+/-}$ and $Stc1^{-/-}$ mice did not exhibit gross morphological or behavioral abnormalities compared to wild-type mice. Histological examination by a qualified veterinary pathologist of the lung, heart, liver, kidney, brain, spleen, stomach, small intestine, colon, ovary, uterus, and testis did not reveal overt differences (data not shown).

*Stc1* has been shown to be highly expressed in osteoblasts and chondrocytes, and a role in bone development has been suggested (13, 32). Skeletal X-ray analyses on wild-type and $Stc1^{-/-}$ animals at the age of 4 months and 9 months were performed. No skeletal abnormalities were seen (data not shown) at this level of resolution. To further substantiate this, we also measured whole-body bone mineral content and density and fat content of the mice using dual-energy X-ray absorptiometry (DEXA). No significant differences were seen between $Stc1^{+/+}$ and $Stc1^{-/-}$ mice (Table 1).

**Analysis of reproductive capabilities.** The ovary and testis have been shown to have high levels of *Stc1* mRNA expression (1, 26). In order to determine whether fertility was affected in $Stc1^{-/-}$ mice, multiple matings were carried out. Each pair of $Stc1^{+/+}$ and $Stc1^{-/-}$ mice was housed separately and allowed to mate for 4 months. Pups were separated after weaning. No physical differences were noted between $Stc1^{-/-}$ pups and pups from wild-type mice. Table 2 shows that similar numbers of pups were born and that the average number of pups per

TABLE 1. Body composition analysis of 7-week-old mice measured with DEXA[a]

| Mice[b] (*n*) | Wt (g) | Bone mineral density (mg/cm$^2$) | Bone mineral content (mg) | % Fat |
|---|---|---|---|---|
| Male | | | | |
| WT (6) | 24.4 ± 0.8 | 51.9 ± 1.4 | 353.1 ± 18.0 | 17.5 ± 0.7 |
| Null (8) | 24.4 ± 0.4 | 53.3 ± 0.5 | 377.6 ± 13.7 | 15.9 ± 0.4 |
| Female | | | | |
| WT (13) | 17.8 ± 0.3 | 44.6 ± 0.6 | 287.5 ± 8.0 | 18.9 ± 0.5 |
| Null (10) | 18.2 ± 0.3 | 47.0 ± 1.0 | 309.4 ± 12.5 | 17.4 ± 0.4 |

[a] All values are expressed as the mean ± standard error of the mean.
[b] Wild-type (WT) and *Stc1*-null mice were studied.

TABLE 2. Offspring from multiple matings[a]

| Genotype | No. of pups | | | Total no. of litters | Avg litter size (SD) |
|---|---|---|---|---|---|
| | Female | Male | Total | | |
| +/+ × +/+ | 53 | 66 | 119 | 18 | 6.5 (±2.3) |
| −/− × −/− | 82 | 88 | 170 | 23 | 7.4 (±2.5) |

[a] Five pairs of wild-type (+/+) and mutant (−/−) mice were housed separately and allowed to mate for 4 months. Pups were separated from the parents after weaning.

litter was similar, suggesting that the absence of *Stc1* does not affect the fertility of male or female mice.

**Measurement of serum calcium and phosphorus after vitamin $D_3$ treatment.** As in vitro experiments have suggested that mammalian STC1 has a role in calcium and/or phosphate homeostasis, we induced hypercalcemia by treating with vitamin $D_3$ to determine whether the *Stc1*$^{-/-}$ mice respond differently. *Stc1*$^{-/-}$ and wild-type mice received four daily injections of vitamin $D_3$, and blood serum was collected for calcium and phosphorus measurements. The results (Fig. 7) showed that (i) there was no difference in the normal level of serum calcium and phosphorus in wild-type and *Stc1*-deleted mice and (ii) that vitamin $D_3$ increased the level of calcium and phosphorus

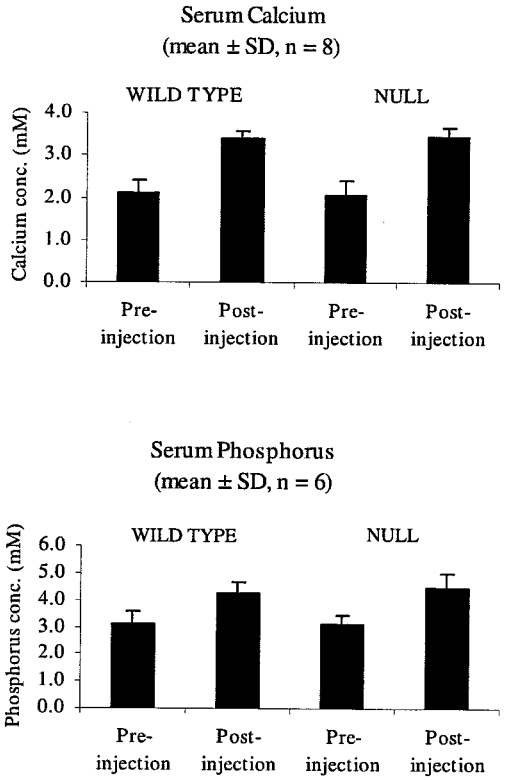


FIG. 7. Measurement of serum calcium and phosphorus concentrations (conc.) in wild-type and homozygous mutant mice. Wild-type and homozygous mutant adult female mice were given intraperitoneal injections of vitamin D3 at a dose rate of 2 μg/kg of body weight daily for 4 days. A small amount of blood was collected from the tail before the start of injections, and terminal blood was taken the morning after the last injections. Bars show mean values, and error bars indicate standard deviations.

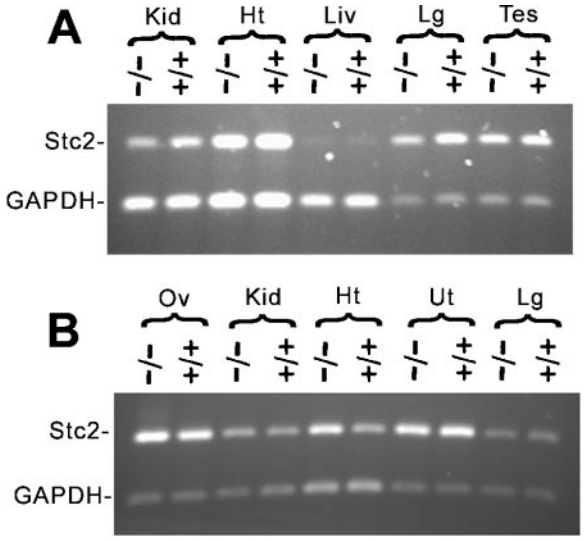


FIG. 8. Analysis of *Stc2* RNA expression. RT-PCR amplification of STC2 from various organs isolated from male (A) and female (B) wild-type (+/+) and homozygous mutant (−/−) mice. Amplification of GAPDH was used as the internal control, with a smaller amount of starting cDNA and fewer cycles of amplification. Kid, kidney; Ht, heart; Liv, liver; Lg, lung; Tes, testis; Ov, ovary; Ut, uterus.

to the same extent regardless of genotype, suggesting that *Stc1* does not have a systemic antihypercalcemic role in this context.

**Treadmill performance.** It has previously been demonstrated that expression of STC1 can be induced by a variety of stress factors, including elevated calcium, hypoxia, traumatic brain injury, and viral infection. To test response to stress, we subjected wild-type and *Stc1*$^{-/-}$ mice to continuous exercise on an exercise treadmill and found that the endurance of *Stc1*$^{-/-}$ mice (11.8 ± 5.6 min [mean ± standard error of the mean]; $n = 7$) was similar to that of wild-type mice (11.8 ± 7.0 min; $n = 4$).

**Analysis of *Stc2* mRNA expression.** To investigate whether *Stc2* mRNA expression could be compensating for the loss of *Stc1*, total RNA was isolated from organs that normally express *Stc1* at a wide range of levels and was analyzed by RT-PCR (1, 26). No consistent up-regulation of *Stc2* mRNA expression was seen in *Stc1*$^{-/-}$ ovary, kidney, testis (organs known to express high levels of *Stc1*), heart, lung, uterus (low *Stc1* expression) or liver (undetectable *Stc1* expression) compared with *Stc1*$^{+/+}$ organs (Fig. 8).

## DISCUSSION

We isolated the *Stc1* gene from a mouse strain 129 genomic library and sequenced the complete gene, which has four exons. Two independent lines of mutant mice were generated in which *Stc1* exons 2 and 3 and the protein-coding portion of exon 1 were deleted. Southern and Northern blot analyses showed that the expected deletion had occurred. Deletion of *Stc1* was further confirmed by Western blot analysis showing the absence of the 32-kDa STC1 protein from the quadriceps of *Stc1*$^{-/-}$ mice. In some tissues, including kidney and heart, the polyclonal antibody cross-reacted with larger proteins. Many groups, including our own, have reported immunohisto-

chemical analyses of STC1 expression, and the cross-reactivity seen here highlights the importance of using gene-deleted tissue samples as negative controls in such studies.

*Stc1* expression has been reported in a variety of tissues during early mouse development, especially the skeletal and muscular tissues (13, 24, 31). Mice that overexpressed a human STC1 transgene (driven by exogenous metallothionein promoter or myosin light-chain promoter) were dwarfed and had decreased bone length (7, 25). It was therefore unexpected that our *Stc1*$^{-/-}$ mice were born apparently healthy without overt abnormalities and grew at a rate that was indistinguishable from that of wild-type mice. Some of the mutant mice have been kept for over 20 months with no apparent abnormalities. Skeletal X-rays and DEXA analyses of mineral content were also normal. Thus, although overexpressed ectopic STC1 in transgenic mice negatively regulates growth, growth is essentially normal in the absence of *Stc1*.

The ovary is the site of greatest *Stc1* expression in mature mice (1), and it has been reported that *Stc1* is highly expressed in theca-interstitial cells of the ovary, in the corpora lutea, and in the oocyte (26). In addition, ovarian STC1 production increases during gestation and the presence of a nursing litter results in increased expression in lactating mice (5), and STC1 is found in mammary gland ductal epithelium (28). These data have been interpreted to suggest that STC1 is involved in regulation of ovarian function and lactation. Furthermore, it has been shown that transgenic female mice overexpressing STC1 had severely compromised reproductive ability, and wild-type pups nursed by transgenic mothers were underweight (25). However, the *Stc1*$^{-/-}$ mice had no alteration in fecundity, with no decrease in litter number or size. Pups of *Stc1*$^{-/-}$ mothers had normal weight at weaning. The data therefore indicate that lack of *Stc1* function did not have a significant adverse effect on either reproductive ability or lactation.

Several early reports using recombinant protein suggested that mammalian STC1 might have conserved the antihypercalcemic role previously documented for fish STC (19, 21, 27). We chose to induce hypercalcemia in the *Stc1*$^{-/-}$ mice by treatment with vitamin $D_3$, in part because its active metabolite has been shown to increase *Stc1* mRNA levels in mouse and rat kidneys (10, 29). We found that the levels of serum calcium and phosphate were identical to those of similarly treated wild-type animals. This observation suggests that mammalian STC1 may not have a major systemic role in controlling the serum calcium level, at least when it is perturbed by vitamin $D_3$. This is consistent with a recent report on transgenic mice that contained high blood levels of human STC1 protein but were nevertheless normocalcemic (25). However, in view of the data showing that administration of STC1 can affect mineral homeostasis and the observation that one out of two transgenic mouse models overexpressing human STC1 were hyperphosphatemic, more-extensive studies of calcium and phosphate metabolism in the *Stc1*$^{-/-}$ mice are warranted.

Our data suggest that under normal laboratory housing conditions, in a pathogen-reduced environment, mice lacking STC1 can develop normally; however, it is clear from previous studies that STC1 production can be induced by a wide variety of stresses, including hypoxia and viral infection. In view of data indicating that *Stc1* transgenic mice have musculoskeletal abnormalities, including abnormal muscle mitochondria (7), we examined the responses of wild-type and *Stc1*$^{-/-}$ mice to the mild stress of exercise on a treadmill. We did not find any alteration in the endurance of the *Stc1*$^{-/-}$ mice, but these mice are an excellent model system for investigating the possibility that *Stc1* has a role in response to other types of stress.

Mammals and fish contain a second stanniocalcin gene, *Stc2* (4, 6, 11, 18, 20). The STC2 protein has about 35% sequence identity with STC1 and is also expressed in a wide variety of tissues in mice (4, 9, 11). We considered the possibility that the loss of *Stc1* function had been compensated by the expression of *Stc2* and tested this by examining *Stc2* mRNA expression in tissues including kidney, heart, liver, lung, testis, uterus and ovary. No evidence for up-regulation of *Stc2* mRNA was found. To definitively rule out the possibility that *Stc2* expression is able to compensate for the loss of *Stc1* in *Stc1*$^{-/-}$ mice, it will be necessary to generate mice that are null for both *Stc1* and *Stc2*.

## ACKNOWLEDGMENTS

This work was supported by a project grant from the National Health and Medical Research Council of Australia and by a Carcinogenesis Fellowship of the Cancer Council New South Wales.

We thank Irma Villaflor and the other members of the Bioservices Unit of the Children's Medical Research Institute for their help in managing the animals, and we thank L. Barnett, J. DeWinter, and A. Steptoe of the Walter and Eliza Hall Institute of Medical Research for generating the knockout mice. We thank Craig Godfrey for help with the DEXA machine and Edna Hardeman and members of her laboratory for advice regarding analyses of muscle phenotype. We also thank Graham Wagner and Gabe DiMattia for comments on the manuscript.

## REFERENCES

1. **Chang, A. C. M., M. A. Dunham, K. J. Jeffrey, and R. R. Reddel.** 1996. Molecular cloning and characterization of mouse stanniocalcin cDNA. Mol. Cell. Endocrinol. **124:**185–187.
2. **Chang, A. C. M., J. Janosi, M. Hulsbeek, D. De Jong, K. J. Jeffrey, J. R. Noble, and R. R. Reddel.** 1995. A novel human cDNA highly homologous to the fish hormone stanniocalcin. Mol. Cell. Endocrinol. **112:**241–247.
3. **Chang, A. C. M., D. A. Jellinek, and R. R. Reddel.** 2003. Mammalian stanniocalcins and cancer. Endocr. Relat. Cancer **10:**359–373.
4. **Chang, A. C. M., and R. R. Reddel.** 1998. Identification of a second stanniocalcin cDNA in mouse and human: stanniocalcin 2. Mol. Cell. Endocrinol. **141:**95–99.
5. **Deol, H. K., R. Varghese, G. F. Wagner, and G. E. DiMattia.** 2000. Dynamic regulation of mouse ovarian stanniocalcin expression during gestation and lactation. Endocrinology **141:**3412–3421.
6. **DiMattia, G. E., R. Varghese, and G. F. Wagner.** 1998. Molecular cloning and characterization of stanniocalcin-related protein. Mol. Cell. Endocrinol. **146:**137–140.
7. **Filvaroff, E. H., S. Guillet, C. Zlot, M. Bao, G. Ingle, H. Steinmetz, J. Hoeffel, S. Bunting, J. Ross, R. A. Carano, L. Powell-Braxton, G. F. Wagner, R. Eckert, M. E. Gerritsen, and D. M. French.** 2002. Stanniocalcin 1 alters muscle and bone structure and function in transgenic mice. Endocrinology **143:**3681–3690.
8. **Fontaine, M.** 1964. Stannius' corpuscles and ionic (Ca, K, Na) of the interior environment of the eel (*Anguilla anguilla* L.). C. R. Acad. Sci. D **259:**875–878.
9. **Gagliardi, A. D., E. Y. Kuo, S. Raulic, G. F. Wagner, and G. E. DiMattia.** 2005. Human stanniocalcin-2 exhibits potent growth suppressive properties in transgenic mice independent of growth hormone and IGFs. Am. J. Physiol. Endocrinol. Metab. **288:**E92–E105.
10. **Honda, S., M. Kashiwagi, K. Ookata, A. Tojo, and S. Hirose.** 1999. Regulation by 1α,25-dihydroxyvitamin $D_3$ of expression of stanniocalcin messages in the rat kidney and ovary. FEBS Lett. **459:**119–122.
11. **Ishibashi, K., K. Miyamoto, Y. Taketani, K. Morita, E. Takeda, S. Sasaki, and I. Imai.** 1998. Molecular cloning of a second human stanniocalcin homologue (STC2). Biochem. Biophys. Res. Commun. **250:**252–258.
12. **Jellinek, D. A., A. C. Chang, M. R. Larsen, X. Wang, P. J. Robinson, and R. R. Reddel.** 2000. Stanniocalcin 1 and 2 are secreted as phosphoproteins from human fibrosarcoma cells. Biochem. J. **350:**453–461.
13. **Jiang, W. Q., A. C. M. Chang, M. Satoh, Y. Furuichi, P. P. Tam, and R. R.**

**Reddel.** 2000. The distribution of stanniocalcin 1 protein in fetal mouse tissues suggests a role in bone and muscle development. J. Endocrinol. **165:**457–466.
14. **Kahn, J., F. Mehraban, G. Ingle, X. Xin, J. E. Bryant, G. Vehar, J. Schoenfeld, C. J. Grimaldi, F. Peale, A. Draksharapu, D. A. Lewin, and M. E. Gerritsen.** 2000. Gene expression profiling in an *in vitro* model of angiogenesis. Am. J. Pathol. **156:**1887–1900.
15. **Kanellis, J., R. Bick, G. Garcia, L. Truong, C. C. Tsao, D. Etemadmoghadam, B. Poindexter, L. Feng, R. J. Johnson, and D. Sheikh-Hamad.** 2003. Stanniocalcin-1, an inhibitor of macrophage chemotaxis and chemokinesis. Am. J. Physiol. Renal Physiol. **286:**F356–F362.
16. **Lafeber, F. P., G. Flik, S. E. Wendelaar Bonga, and S. F. Perry.** 1988. Hypocalcin from Stannius corpuscles inhibits gill calcium uptake in trout. Am. J. Physiol. **254:**R891–R896.
17. **Lu, M., G. F. Wagner, and J. L. Renfro.** 1994. Stanniocalcin stimulates phosphate reabsorption by flounder renal proximal tubule in primary culture. Am. J. Physiol. **267:**R1356–R1362.
18. **Luo, C. W., M. D. Pisarska, and A. J. Hsueh.** 2004. Identification of a Stanniocalcin paralog, STC2, in fish and the paracrine actions of STC2 in the mammalian ovary. Endocrinology **146:**469–476.
19. **Madsen, K. L., M. M. Tavernini, C. Yachimec, D. L. Mendrick, P. J. Alfonso, M. Buergin, H. S. Olsen, M. J. Antonaccio, A. B. Thomson, and R. N. Fedorak.** 1998. Stanniocalcin: a novel protein regulating calcium and phosphate transport across mammalian intestine. Am. J. Physiol. **274:**G96–G102.
20. **Moore, E. E., R. E. Kuestner, D. C. Conklin, T. E. Whitmore, W. Downey, M. M. Buddle, R. L. Adams, L. A. Bell, D. L. Thompson, A. Wolf, L. Chen, M. R. Stamm, F. J. Grant, S. Lok, H. Ren, and K. S. De Jongh.** 1999. Stanniocalcin 2: characterization of the protein and its localization to human pancreatic alpha cells. Horm. Metab. Res. **31:**406–414.
21. **Olsen, H. S., M. A. Cepeda, Q. Q. Zhang, C. A. Rosen, B. L. Vozzolo, and G. F. Wagner.** 1996. Human stanniocalcin: a possible hormonal regulator of mineral metabolism. Proc. Natl. Acad. Sci. USA **93:**1792–1796.
22. **Sato, N., K. Kokame, K. Shimokado, H. Kato, and T. Miyata.** 1998. Changes of gene expression by lysophosphatidylcholine in vascular endothelial cells: 12 up-regulated distinct genes including 5 cell growth-related, 3 thrombosis-related, and 4 others. J. Biochem. **123:**1119–1126.
23. **Shalaby, F., J. Rossant, T. P. Yamaguchi, M. Gertsenstein, X. F. Wu, M. L. Breitman, and A. C. Schuh.** 1995. Failure of blood-island formation and vasculogenesis in Flk-1-deficient mice. Nature **376:**62–66.
24. **Stasko, S. E., and G. F. Wagner.** 2001. Possible roles for stanniocalcin during early skeletal patterning and joint formation in the mouse. J. Endocrinol. **171:**237–248.
25. **Varghese, R., A. D. Gagliardi, P. E. Bialek, S. P. Yee, G. F. Wagner, and G. E. DiMattia.** 2002. Overexpression of human stanniocalcin affects growth and reproduction in transgenic mice. Endocrinology **143:**868–876.
26. **Varghese, R., C. K. Wong, H. Deol, G. F. Wagner, and G. E. DiMattia.** 1998. Comparative analysis of mammalian stanniocalcin genes. Endocrinology **139:**4714–4725.
27. **Wagner, G. F., B. L. Vozzolo, E. Jaworski, M. Haddad, R. L. Kline, H. S. Olsen, C. A. Rosen, M. B. Davidson, and J. L. Renfro.** 1997. Human stanniocalcin inhibits renal phosphate excretion in the rat. J. Bone Miner. Res. **12:**165–171.
28. **Welcsh, P. L., M. K. Lee, R. M. Gonzalez-Hernandez, D. J. Black, M. Mahadevappa, E. M. Swisher, J. A. Warrington, and M. C. King.** 2002. BRCA1 transcriptionally regulates genes involved in breast tumorigenesis. Proc. Natl. Acad. Sci. USA **99:**7560–7565.
29. **Yahata, K., K. Mori, M. Mukoyama, A. Sugawara, T. Suganami, H. Makino, T. Nagae, Y. Fujinaga, Y. Nabeshima, and K. Nakao.** 2003. Regulation of stanniocalcin 1 and 2 expression in the kidney by klotho gene. Biochem. Biophys. Res. Commun. **310:**128–134.
30. **Yang, B., J. M. Verbavatz, Y. Song, L. Vetrivel, G. Manley, W. M. Kao, T. Ma, and A. S. Verkman.** 2000. Skeletal muscle function and water permeability in aquaporin-4 deficient mice. Am. J. Physiol. Cell Physiol. **278:**C1108–C1115.
31. **Yoshiko, Y., J. E. Aubin, and N. Maeda.** 2002. Stanniocalcin 1 (STC1) protein and mRNA are developmentally regulated during embryonic mouse osteogenesis. The potential of STC1 as an autocrine/paracrine factor for osteoblast development and bone formation. J. Histochem. Cytochem. **50:**483–492.
32. **Yoshiko, Y., A. Son, S. Maeda, A. Igarashi, S. Takano, J. Hu, and N. Maeda.** 1999. Evidence for stanniocalcin gene expression in mammalian bone. Endocrinology **140:**1869–1874.
33. **Zhang, K., J. A. Westberg, A. Paetau, K. von Boguslawsky, P. Lindsberg, M. Erlander, H. Guo, J. Su, H. S. Olsen, and L. C. Andersson.** 1998. High expression of stanniocalcin in differentiated brain neurons. Am. J. Pathol. **153:**439–445.
34. **Zlot, C., G. Ingle, J. Hongo, S. Yang, Z. Sheng, R. Schwall, N. Paoni, F. Wang, F. V. Peale, Jr., and M. E. Gerritsen.** 2003. Stanniocalcin 1 is an autocrine modulator of endothelial angiogenic responses to hepatocyte growth factor. J. Biol. Chem. **278:**47654–47659.